Aalto University

OPEN ACCESS

This is an electronic reprint of the original article.
This reprint may differ from the original in pagination and typographic detail.

Lepikko, Sakari; Miettunen, Kati; Poskela, Aapo; Tiihonen, Armi; Lund, Peter D.

Testing dye-sensitized solar cells in harsh northern outdoor conditions

Published in:
Energy Science and Engineering

DOI:
10.1002/ese3.195

Published: 01/06/2018

Document Version
Publisher's PDF, also known as Version of record

Published under the following license:
CC BY

Please cite the original version:
Lepikko, S., Miettunen, K., Poskela, A., Tiihonen, A., & Lund, P. D. (2018). Testing dye-sensitized solar cells in harsh northern outdoor conditions. *Energy Science and Engineering*, *6*(3), 187-200. https://doi.org/10.1002/ese3.195

This material is protected by copyright and other intellectual property rights, and duplication or sale of all or part of any of the repository collections is not permitted, except that material may be duplicated by you for your research use or educational purposes in electronic or print form. You must obtain permission for any other use. Electronic or print copies may not be offered, whether for sale or otherwise to anyone who is not an authorised user.

Energy Science & Engineering

Open Access

RESEARCH ARTICLES

Testing dye-sensitized solar cells in harsh northern outdoor conditions

Sakari Lepikko[1], Kati Miettunen[1,2], Aapo Poskela[1], Armi Tiihonen[1] & Peter D. Lund[1]

[1]New Energy Technologies Group, Department of Applied Physics, Aalto University, P.O.B. 15100, FI-00076, Aalto, Finland
[2]Biobased Colloids and Materials, Department of Bioproducts and Biosystems, Aalto University, P.O.B. 16300, FI-00076, Aalto, Finland

Keywords
Aging, degradation, lifetime, photovoltaics, stability

Correspondence
Kati Miettunen, Biobased Colloids and Materials, Department of Bioproducts and Biosystems, P.O.B. 16300, FI-00076 Aalto, Finland. E-mail: kati.miettunen@aalto.fi

Funding Information

Academy of Finland (Grant/Award Number: 271081); Tiina and Antti Herlin Foundation; Koneen Säätiö.

Received: 2 February 2018; Revised: 15 March 2018; Accepted: 17 April 2018

doi: 10.1002/ese3.195

Abstract

Here, we report on the behavior of dye solar cells in real-life weather conditions from a northern outdoor test covering for the first time cell performance measurements in harsh conditions with varying weather from mildly warm conditions to freezing and snowy. The effect of different weather conditions on the cell performance is quantitatively investigated by using correlations coefficients of weather parameters to cell performance. No degradation was observed during the frosty period, but instead during the warmer, rainy periods with high moisture levels. Nevertheless, after 6 weeks of outdoor testing in varying harsh conditions, the cells maintained on average 88% of their initial efficiency. Tracking the cell performance during the aging showed that the test cells generated roughly as much current at subzero temperatures as at warmer temperatures. Investigations of the degradation reactions revealed that while photoelectrode degradation was the main cause of degradation during this test, the loss of charge carriers, which had only a minor effect on performance during the test, would likely become a major degradation factor during the next 1000 h of testing. Furthermore, the test showed that the cells even doubled their efficiency in low light intensity conditions compared with the standard reporting conditions. Thus, the overall conversion efficiency during the whole experiment reached up to 50% higher values compared with the results in standard testing conditions.

Introduction

Dye-sensitized solar cells (DSSCs) have two performance related advantages compared to crystalline silicon (c-Si) solar cells: (1) their electricity production decreases less than in c-SI with low light intensity [1]; and (2) their electricity production may even increase when temperature rises from warm to hot (>60°C) whilst in silicon solar cells, the electricity production decreases [2]. It has been shown that standard reporting conditions favor silicon solar cells, and in real use, the power output from DSSCs is much closer to that of silicon solar cells than what could be expected based on measurements in standard reporting conditions [1, 3, 4]. Therefore, complimenting laboratory tests with tests in real outdoor conditions is important.

Besides getting the real performance right, going to outdoor testing is important also in regards to stability testing. Understanding the degradation phenomena of dye solar cells has been an issue for the scientific community [5]. Typically, stability studies for solar cells are performed in laboratory conditions using accelerated aging tests. This improves comparability of different stability studies and keeps the investigations fast paced. Usually, the accelerated aging tests are performed in stable conditions or a set of alternating conditions so they may not fully predict the effects caused by weather variations. Thus, outdoor tests can reveal degradation mechanisms that were not foreseen in laboratory aging tests. On the other hand, outdoor studies could also reveal positive surprises. For instance, it has been suggested that the cells revive to some extent when they are taken from illumination to dark [6]. Such variations are a natural part of everyday life and the cells could actually live longer in outdoor conditions than what has been implied by the indoor

© 2018 The Authors. *Energy Science & Engineering* published by the Society of Chemical Industry and John Wiley & Sons Ltd.
This is an open access article under the terms of the Creative Commons Attribution License, which permits use, distribution and reproduction in any medium, provided the original work is properly cited.

testing. To improve the quality of solar cell studies, the cells and materials that performed successfully under simulated conditions should be tested under real outdoor conditions to see, whether the tested cells or materials are stable in outdoors as well.

After Grätzel introduced the DSSC technology, only a handful of reports actually show testing of DSSC outdoors [3, 4, 7–17]. In general, outdoor testing is quite rare for the third generation photovoltaics, for instance regarding perovskite solar cells only two studies were found and both were quite short (days to weeks) [18, 19]. Mostly, the DSSC outdoor studies demonstrate manufacturing a module with larger size and its ability to function in power generation, but there are also studies of single cells. The typical aging time scale is several months [4, 7–11], but there are also studies where cells have been outdoors for only few days to weeks [3, 12, 13, 17–19] or much longer tests from one to 2.5 years [14, 15]. Locations of the studies limit on rather narrow longitude range from 21°N to 48°N (Table 1) and studies are mostly rather close to sea level with maximum altitude around 300 m. The typical climate conditions are subtropical and mostly sunny, ranging from dry to humid.

There are standards/protocols for outdoor testing that can be used as the basis for the investigation of DSSCs: ISOS protocol, which is designed for the organic solar cells, and IEC standards, which are for thin film solar cells [20]. The ISOS standard is meant for research purposes and, to make aging studies accessible, it contains recommendations for different levels of testing from basic to advanced. The ISOS standard describes the measurement setup in detail: The test cells should face toward the equator and be at tilt angle dependent on the latitude of the test location. A tracking system may also be used. For all levels of outdoor testing, at least ambient and cell temperature, relative humidity, and solar irradiance have to be recorded.

Most outdoor tests found in literature do not comply with these standards but there is more variation in the applied methods. Only three outdoor studies report recording both irradiance and temperatures [3, 7, 17]. Sometimes, only average, maximum, and minimum temperature of cells during the measurements are presented [4, 8, 14]. Humidity is reported only in one study [17]. The advanced level (ISOS-O-3) standard also requires monitoring of wind speed and direction – this has not been done in any of the studies. We also found it difficult to realize in practice, in particular for individual small cells. This is because the cells are attached to a platform, which acts as a windshield – therefore placing an anemometer next to the platform would not actually track the same wind speed that the cells experience. Besides tracking the weather conditions, it is important to consider the operational state of the cells. To best reflect the operational conditions as suggested in the ISOS-O-3 standard, the cells should be kept in at the maximum power state: eight studies [3, 7, 8, 11, 13–16] had the cells or panels operating at maximum power point and two of them [7, 8] had another set of cells at open circuit. Many studies also fail to report the operation regime of the tested cell

Table 1. Descriptions of the study locations. Altitude data [29], global horizontal irradiance (GHI) [30] and climate descriptions [31] are presented for each location. If the time of study is reported, the climate description is limited for that time of the year. Otherwise, the description for climate is the average of the year. The aging tests are focused on warm climates.

Location	Coordinates	Altitude (m)	GHI (kWh/m^2)	Climate description	Times and lengths of study	Ref.
Freiburg im Breisgau, Germany	48°N, 8°E	200–300	1197	Inland, warm, slightly humid, sunny	Summer 3 months	[4]
Ljubljana, Slovenia	46°N, 14°E	200–300	1269	Inland, warm, humid, sunny	April to October	[7]
Turin, Italy	45°N, 7°E	200–300	1389	Inland, warm, humid, partly cloudy	February to April	[9]
Rome, Italy	41°N, 12°E	0–100	1603	Coastal, warm, dry to humid, sunny	–	[3, 8]
Porto, Portugal	41°N, 8°W	0–100	1587	Coastal, warm, dry, sunny	Summer 47 days	[13]
Cheonan, South Korea	37°N, 127°E	50–200	1451	Coastal, warm, very humid, part cloudy	–	[12]
Toyota, Japan	35°N, 137°E	0–100	1499	Coastal, warm, very humid, part cloudy	4 months to 2.5 years	[10, 11, 14, 16]
Hefei, China	32°N, 117°E	0–50	1315	Inland, warm, humid, part cloudy	Full year	[15]
Abi Dhabi, UAE	24°N, 55°E	0–50	2172	Coastal, hot, dry, very sunny	–	[17]

© 2018 The Authors. *Energy Science & Engineering* published by the Society of Chemical Industry and John Wiley & Sons Ltd.

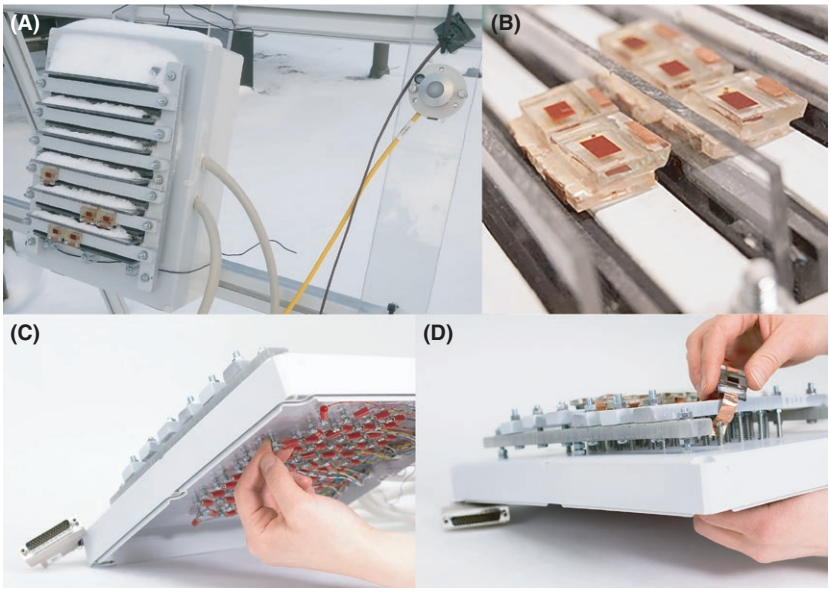

Figure 1. (A) The outdoor station. The cell platform is on the left, and pyranometer and one cell temperature simulating sensor is on the right. (B) The cells connected to their platform and between the cells there are partitioning walls and ledges pressed tightly to these walls to prevent water penertrating into the platform. (C) The electrical connectors are underneath the platform and thus protected from rain and moisture. (D) The electrical connectors have springs with which the cells can be attached to the platform.

or panel during the test, which is a major deficiency. On a positive note, IV measurements for the cells or panels are mostly performed regularly and often enough [3, 4, 7–10, 13–15, 17] which is a key issue listed also in ISOS standards.

In the outdoor studies reported in the literature, the cells were quite well encapsulated from the environment. In three studies, the cells were placed into waterproof, UV filtered containers or other waterproof encapsulations [7, 11, 14]. These covers do not let rainwater get close to the cells and may have a strong greenhouse effect on ambient temperature. In studies [4, 8, 12, 13, 15, 16], the sealed cells were "sandwiched" between two glass plates to form panels. This type of encapsulation is the same or very similar as commercial solar panel encapsulation. In studies [3, 9, 17], cells were exposed for outdoor conditions with minimal weather protection, which enabled measuring the cell during rainy conditions as well. When thinking of encapsulation, it is important to consider which level of encapsulation is viable for commercial devices. This depends on the application. For instance, a 10 mm thick external casing is not viable in lightweight and flexible applications. The encapsulation could significantly affect the light spectrum, for example,by filtering of UV light. Thus, using an overly thick cover may give too positive outlook on the outdoor performance. Naturally, if the covering is of commercially viable level, additional benefits such as UV filtering are not an issue.

In order to complement the previous outdoor tests, here we investigate a northern location, Espoo, Finland (60.2°N, 24.8°E) during late autumn at very humid conditions and partly sub-zero temperature. Of particular interest were the effects of rain and snow, to which reason we prepared outdoor testing unit, which did not utilize any additional coverage. The measurements were automated to decrease the amount of required manual work during aging. The cells were investigated indoors in standard conditions on weekly basis, but the performance was tracked continuously when the cells were kept outdoors.

Experimental

The measurement setup for the outdoor aging

The testing period for the cells was from 6th of October 2016 until 17th of November 2016, which is about 1000 h. The tilt angle of the cells was set to 70° that is about the optimal angle for autumn and wintertime in Espoo, Finland (60.2°N, 24.8°E) and its azimuth was toward south. The installed sensors were pyranometer (SP Lite2; Kipp & Zonen, Delft, Netherlands) for recording solar irradiance, humidity sensor (HM1500LF; TE Connectivity, Schaffhausen, Switzerland) and T-type thermocouples for measuring ambient and cell temperature. The pyranometer was positioned in the same tilt angle as the cells, see

© 2018 The Authors. *Energy Science & Engineering* published by the Society of Chemical Industry and John Wiley & Sons Ltd.

Figure 1A. IV curves of the cells and weather parameters were recorded every 15 min. The weather parameters were recorded just before each IV measurement so that the recorded weather values match as well as possible to the weather conditions during the IV measurements.

The humidity sensor of the setup was connected to the cell platform in such a way that it was protected from rain. The thermocouples measuring air temperature were positioned close to the cells so that they were constantly in the shadow. The thermocouples measuring cell temperature were not physically connected to the cells themselves. Instead, they were positioned to the sun light next to the cells and let heat up due to the irradiation. According to an infrared camera (InfraCAM Wester, FLIR), the thermocouples were approximately in the same temperature than the cells (±2°C, measured on a sunny day October 6th). Thermocouples were not directly connected to the cells since the weather encapsulation of the thermocouples would have limited the heat flow from the cells to the sensors. There were two thermocouples measuring each temperature for the sake of reliability.

One practical issue is to enable the continuous tracking of the IV performance without using an overall coverage to block the rainwater from short-circuiting the system. This kind of system allows the selection of protective coverage case by case – or as here, not having any additional coating to take the stress to the maximum. This ended up being a highly non-trivial problem and hence, we share our solution, which was to have spring terminals beneath the cells and protect them from water by building a comp like structure around them. Firstly, underneath each plastic beam a plastic wall was added which separated the positive and negative terminals. This prevents short-circuiting the cells. Then, each terminal was separated from a neighboring one with a plastic partition wall. Without the partition wall, the neighboring cells could be electrically connected by rainwater. All the walls were sealed with silicon paste so that water cannot pass through the gaps between the walls and the platform. Each photoelectrode spring terminal was separated from the corresponding counter electrode spring terminal (Fig. 1C) with a detachable plastic sheet (Fig. 1B) in order to enable easy cell connection and detachment. Finally, the partition walls were pressed against the beam and comp structure with wedges. The rubber sealant stripes perfect the sealing by making an elastic watertight seal around the copper tape of the solar cell, see Figure 1B. The walls were low enough to not shade the cells at any time of the year with practical tilt angles.

The cells were attached to a platform that was connected to outdoor located aluminum stand with an adjustable tilt angle. The cabling was directed to a stationary connector terminal next to the measurement stand outdoors. The measurement instruments and the computer were located in the nearest indoor laboratory space. The connector terminal is connected to the measurement equipment with 18 m long 44 wire D-sub extension cables. The cable wires were solid copper, which retains a small total wire resistance and the remaining effect of the cable resistance was removed from the IV curves with the measurement program in real time. Additionally, the cables have aluminum foil shielding to block electrical noise entering the cables along the extension wires even though the wires pass some technical spaces with 50 Hz 230 V grid electricity wires. To measure the cell performance, we used a source measure unit (SMU; Keysight U2722A, Santa Rosa, California, USA) and as a switch unit we used Agilent 34980A (Santa Rosa, California, USA) Multifunction Switch Unit. Both instruments were controlled by computer with LabVIEW environment. The cells were kept in open-circuit conditions during the test due to limitations by the automated measurement system. The IV curve was recorded from −0.1 V onwards until the output current passed −0.1 mA. Electrochemical solar cells such as DSSCs have limited response speed to load voltage changes, that is, the current output of the cells takes some time to stabilize after the voltage change. For this reason, the IV scan cannot be performed very fast. For DSSCs, the scan can be performed about in 30–60 sec per scan direction depending on cell structure and degradation state of the cell. The irradiance can vary much quicker than this, so calculating, for example, the efficiency can be a problem. To identify if the measurement conditions had remained constant, the IV scan is performed once in both forward and reverse directions in the program. Especially, on partly cloudy conditions, the irradiance level varies often quickly. This varies the output current of the solar cell, which can be seen easily from an IV scan, see Figure 2. For this reason, both scans are saved so that these kinds of failed scans can be filtered out with least squares method.

Cell assembly

Five laboratory scale solar cells were fabricated for testing the new aging system. The active photoanode area of the cells was 0.4 cm^2 and the total area about 4 cm^2. The cell geometry used included additional area next to the photoelectrode to track changes in the electrolyte color. Loss of charge carriers, seen as electrolyte bleaching, is in literature a major cause of degradation [21]. This setup is not, however, optimal for high performance.

The photoanode of the cell was prepared with screen printing method on an FTO glass plate, which was cleaned thoroughly with washing detergent, ethanol and acetone. In addition, the plate was placed under strong UV light for 20 min in UV-ozone device (UV/Ozone Pro Cleaner;

 © 2018 The Authors. *Energy Science & Engineering* published by the Society of Chemical Industry and John Wiley & Sons Ltd.

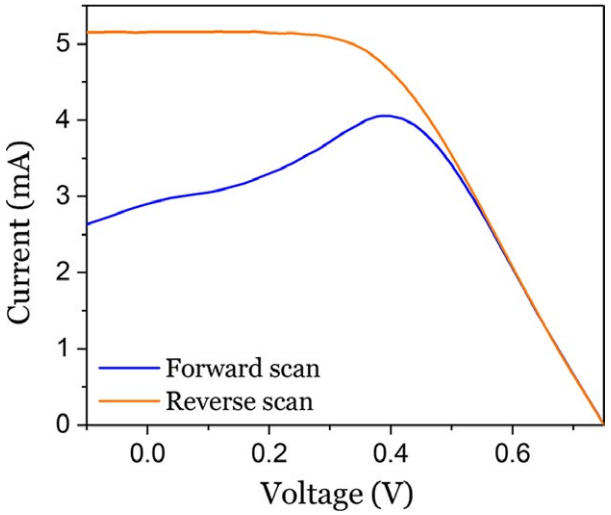

Figure 2. An example of an IV scan where a cloud covered the Sun in the beginning of a scan but not in the end.

BioForce Nanosciences) and then into ultrasonic bath of ethanol for 8 min. The cleaned plate was inserted into a solution of titanium (IV) chloride tetrahydrofuran complex (1 w-%) in de-ionized water and heated for 30 min at 70°C. Next, three rectangular layers of TiO_2 were screen printed on the conductive side of the glass plate. The first two layers contained particles of average size 20 nm (DyeSol (nowadays GreatCell Solar), Queanbeyan, New South Wales, Australia, 18NR-T) and the third layer contained particles of size 150–250 nm (DyeSol, WER2-O). The screen-printed glass plate with TiO_2 layers was sintered for 30 min at 450°C. Another $TiCl_4$ treatment was made after the sintering, similar to the first one, and then the electrodes were sintered once more for 30 min at 450°C. Finally, the pieces were placed into a dye solution that contained Z907 dye (cis-Bis(4,4'-dicarboxy-2,2'-bipyridine) di-isothiocyanato-Ruthenium(II)), and 1:1 acetonitrile and tert-butylalcohol as solvent. The electrodes were dyed for 24 h in dark, airtight container at room temperature.

The counter electrodes were also prepared on FTO glass. 4.0 μL of 5 mmol/L H_2PtCl_6 in 2-propanol solvent was spread with micro-pipette evenly over the conductive side of the glass piece. The coated pieces were sintered for 20 min at 390°C. The counter electrode had filling holes for the electrolyte. The two electrodes were attached to each other with a 20 μm thick Surlyn® thermoplastic foil, which was placed between the electrodes and then heated for 1 min at 120°C. After that the electrolyte was inserted into the cells. The electrolyte consisted of 1-methyl-benzimidazole (NMBI), 1-propyl-3-methylimidazolium (PMII), and iodine (I_2) dissolved into 3-methoxypropionitrile (MPN). The ratios of the NMBI, PMII, I_2, and MPN were 5:5:1:10 (mol-%), respectively. The electrolyte filling holes were sealed with another layer of Surlyn foil and a thin cover glass. Then, copper tapes were added as electrical contacts, and the contact between the FTO and the tape was improved with silver paste. Lastly, the electrical contact and the edges of the cells were sealed with epoxy (Strong Epoxy Professional, Casco (part of Sika concern), Spånga, Sweden). The cells were assembled at ambient conditions: temperature around 20°C and relative humidity between 40% and 50%.

Measurements

In addition to monitoring the IV curves outdoor, the cells were characterized with different methods in standard indoor conditions, either on weekly basis or just initially before the outdoor test and afterward it. See Table 2 for summary of the characterization methods and parameters. Before each weekly characterization, the cells were left to dry and warm up until they reached room temperature. The characterization light source for IV and EIS was Peccel PecL01 class A solar simulator. The characterization light for saturation current was in-house built LED light with intensity range 0.4–9 Sun equivalent. Opaque tape mask was applied on top of the cells during the IV and EIS measurements to prevent diffuse light reaching the active area of the cell.

Results and Discussion

Weather during the test

An outdoor aging test was performed for DSSCs. As Figure 3 shows, the weather conditions varied significantly during the test: the weather was first relatively warm and sunny, then 1 week rainy and chilly, 1 week frosty and snowy, and lastly rainy and chilly again. During the snowy period, the cells had occasionally been buried under the snow. Temperature, humidity, and irradiance are shown in Figure 3. The humidity was extremely high throughout the test (Fig. 3). During the test, cumulative irradiance reached only 34 kWh/m^2 that corresponds to 34 h of 1 Sun illumination. This is a small doze of illumination since the cell type used here has proven to be stable for over 800 kWh/m^2 illumination doses in indoor light soaking tests [22].

Indoor measurements

Firstly, we will analyze the indoor measurements done on weekly basis or at the beginning and end of the experiment. Then in the next section, we look into the data measured in outdoor conditions.

Figure 4A illustrates that there are two clear drops in the average cell efficiency η: between weeks 2 and 3 and later between weeks 5 and 6. The efficiency has decreased

© 2018 The Authors. *Energy Science & Engineering* published by the Society of Chemical Industry and John Wiley & Sons Ltd.

Table 2. Summary of characterization methods.

IV	Interval	Weekly
	Device	Keithley 2401
	Light spectrum	AM 1.5 G, 100 mW/cm^2
	Temperature	25 ± 3°C
	Voltage range	−0.3 V to 0.8 V
EIS	Interval	Weekly
	Device	Zhaner Zennium
	Light spectrum	AM 1.5 G, 100 mW/cm^2
	Temperature	40 ± 5°C
	Frequency range	100 mHz to 4 MHz
	Bias DC voltage	Open circuit
Cell photographing	Interval	Weekly
	Device	Olympus E620
	Other settings	See ref. 6
IPCE	Interval	Initial and final
	Device	PV Measurements QEX7
	Temperature	22 ± 3°C
	Light range	400 nm to 1000 nm
Saturation current	Interval	Initial and final
	Device	Autolab PGSTAT N302
	Light spectrum	White LED
	Light range	0.4 sun to 9 sun equivalent
	Temperature	27 ± 3°C
	Voltage range	−0.3 V to 0.8 V

mainly because the cells generate less current. On the other hand, the open circuit voltage V_{OC} increases significantly during the first rainy week. The average fill factor *FF* is more stable, increasing only slightly, mainly due to decreasing current. The cells maintained 88% of their initial efficiency after the test: the initial average cell efficiency of 3.8% had decreased to 3.4%. Note that the cell geometry was designed for aging studies (i.e., leaving additional space to track changes in the electrolyte color) and it is not optimized for high performance.

The weather was rainy (not snowing) at the times when I_{SC} dropped so the extreme moisture very likely caused the degradation of the cells. On the contrary, the cells seem to be stable at sub-zero temperatures. The effect of water on the cell stability has been under debate and the literature presents partly contradictory results. One study reported increased V_{OC} and *FF* as well as decreased I_{SC} similar to this study, although they used hydrophilic N719 dye instead of hydrophobic Z907 employed here [23]. There, it was suggested that water shifts the lower band edge of TiO_2 nanoparticles higher so that less excited electrons are able to move from the LUMO level of the dye to the conduction band of the nanoparticles. This would increase V_{OC}, which is the potential difference between the Fermi level of the TiO_2 and redox electrolyte without any losses. Due to the increased bandgap of TiO_2, I_{SC} would decrease. In another study [24], 10 vol-% water content in the electrolyte slightly increased both I_{SC} and V_{OC} leading to an increased efficiency for the cells dyed with Z907. Furthermore, the study reports that the cells with 10 vol-% water content were stable for 1000 h under simulated sunlight. Another study examined the effect of water on some common dyes [24]. They found that soaking photoanodes with hydrophilic N3 and N719 dyes in water-ethanol solution instead of pure ethanol caused dye desorption unlike with hydrophobic Z907. Again, the cells prepared from water-ethanol soaked photoanodes had higher V_{OC} but lower I_{SC}. It should be noted that all the listed studies added most likely distilled water to the cells – not rainwater, which contains numerous impurities.

The aging data shown here is for three cells. Initially, there were five tested cells but two cells leaked during the experiment and they were left out of final analysis as outliers. It may be that even though the temperature variation, in particular going to sub-zero temperatures and back, was not detrimental for the intrinsic function of the cell, it caused mechanical strain to the sealing of the cells resulting in leakages.

The changes in the internal resistances of the cells were investigated using electrochemical impedance spectroscopy (EIS). Results are shown in Figure 5. After the first rainy week (week 3), the EIS data readability decreased: easily distinguishable semicircles disappeared from Nyquist plots showing thereafter only one wide semicircle (data not shown here). This complicated the fitting of the equivalent circuit to the spectrum, and often the obtained parameters varied significantly between consecutive fits. The fitting difficulties account for the large standard deviation in the EIS results after the third week of the aging test.

Despite of the large uncertainties in the EIS results of Figure 5, the data still shows some clear aging trends. Overall, the average series resistance R_S related to the Ohmic losses in the cells has decreased slightly, while the other resistance components have remained stable within error margins. R_S decreases at the beginning of the test before the rainy week so it is most likely due to the initial stabilization of the cells. Performance increase shortly after the cell assembly is typical for DSSCs although the exact reactions behind the phenomenon are not yet understood. The resistance at the counter electrode/electrolyte interface R_{CE} and the diffusion resistance of the electrolyte R_D remained quite stable, at least for some cells. Thus, the internal resistance may not contribute largely to the cell degradation. This is consistent with the IV measurement data (Fig. 4), where *FF*, which changes arise mainly from the changes in the cell resistances, remained rather constant.

Photos representing the color changes of one of the cells from the beginning to the end of the test are shown

© 2018 The Authors. *Energy Science & Engineering* published by the Society of Chemical Industry and John Wiley & Sons Ltd.

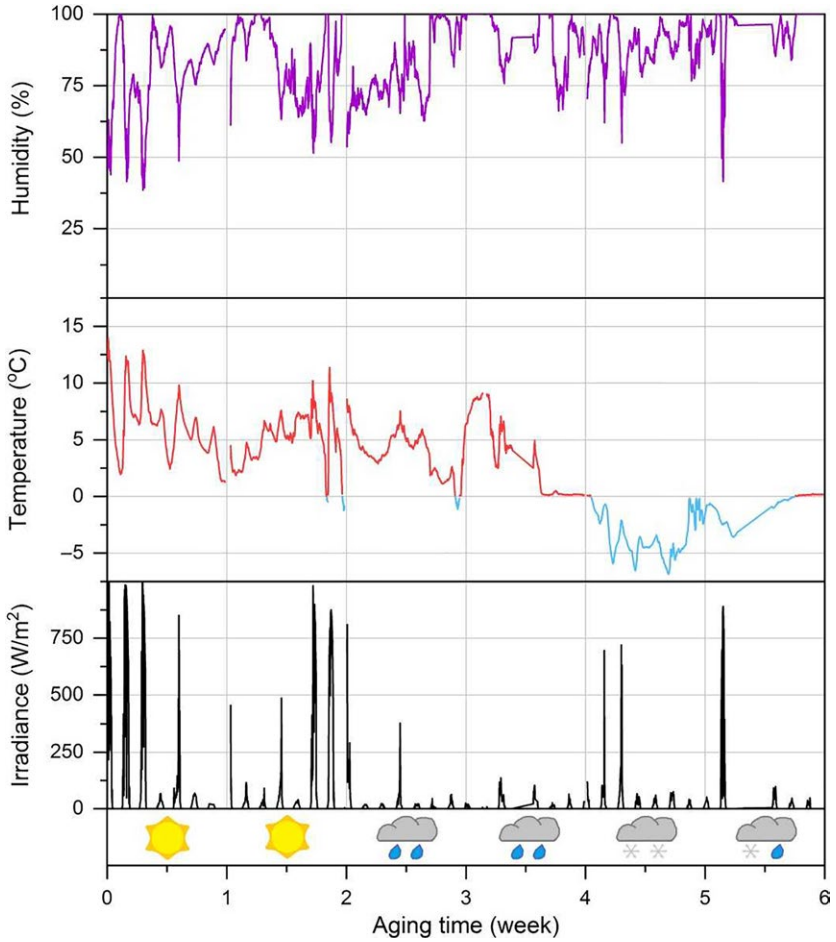

Figure 3. The temperature, humidity, irradiance, and weather type during the test period.

in Figure 6A. The color of the dyed TiO_2 has remained stable during the test period; the variation of RGB values fitting inside the error margins (data not shown). In contrast, the color of the electrolyte changes from yellowish to more transparent. The yellow color of the electrolyte originates from the tri-iodide in the electrolyte, which is the charge carrier that limits the maximal charge transfer in the cells. By tracking the color of the electrolyte, it is possible to evaluate the amount of the tri-iodide in the electrolyte and estimate the changes in the limiting current [6]. The bleaching of the yellow color is visible in the RGB values as an increase of the RGB blue pixel value plotted in Figure 6B. In some cases, as shown in Figure 6A, the color change was not even but there was a color transient: in week 6 the lower part of the cell is almost colorless whereas the upper part of the cell is still light yellow. Similar color transients have been detected in literature and there the effect was suspected to be related to gravity [8]. Initially, the blue pixel value was 70, and after the testing 105. This corresponds to approximately 50% decrease in the iodine concentration from 0.05 to 0.025 mol/L (using the correlation determined in our previous study) [6]. There is an excess of tri-iodide in the fresh electrolyte so such a loss does not limit the photocurrent production at 1 Sun light intensity. This result is in good correspondence with the IV and IPCE data since the changes in the IPCE reflecting losses in the photoelectrode performance were able to explain the decrease of I_{SC}, and losses in the electrolyte discussed here were not contributing the reduced I_{SC}. However, it should be considered that if there was now 50% loss of tri-iodide during the test – continuing the test for another 1000 h in similar conditions would result in a full loss of charge carriers and to a complete failure of these devices. The loss of charge carriers is often related to degradation under UV illumination [6, 21, 25], and even a small cumulative dose could play some role in the bleaching of these cells.

The reduction in the photocurrent production observed in Figure 4 was investigated with incident photon to

© 2018 The Authors. *Energy Science & Engineering* published by the Society of Chemical Industry and John Wiley & Sons Ltd.

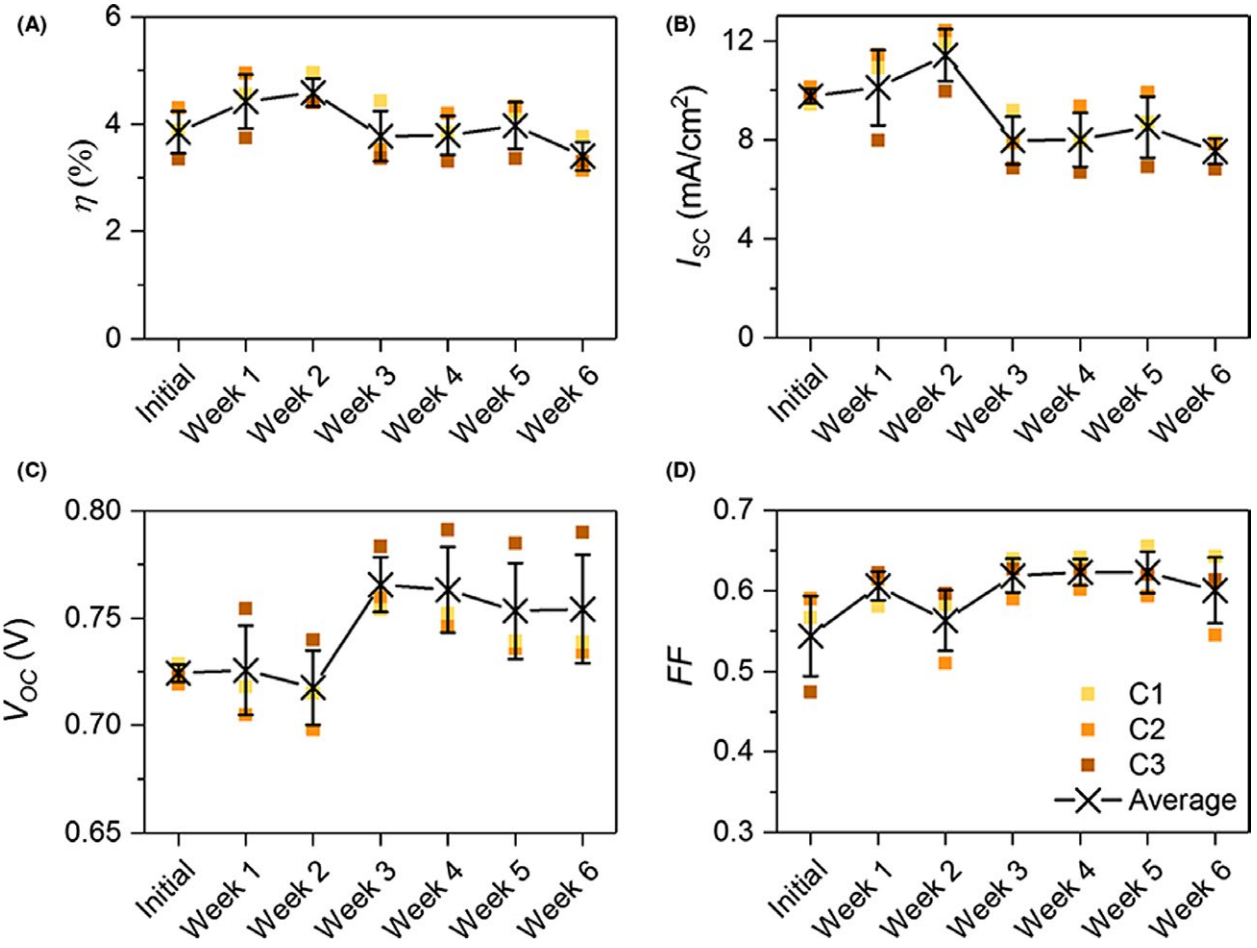

Figure 4. The figure shows (A) efficiency, (B) short circuit current density, (C) open circuit voltage, and (D) fill factor measured under AM 1.5 G spectrum at 1 Sun equivalent at 25°C. The error bars indicate the standard deviation. The drops in the short circuit current and efficiency coincide with the rainy periods (Fig. 3).

collected electron (IPCE) measurements. The reduced I_{SC} can arise from reduced capacity of the photoelectrode to convert photons to electrons, decreased electron collection, or the decreased amount of active charge carriers in the electrolyte. The photoelectrode degradation should affect the performance of the cells rather constantly under any light intensity whereas the loss of charge carriers in the electrolyte should limit the photocurrent more under higher than lower light intensities. Here, the IPCE measurements shown in Figure 7 were carried out without bias light under low light intensity. IPCE had decreased on average about 30% during the aging test, which is about the same relative drop as in I_{SC} (Fig. 4A). Now that the decrease in I_{SC} measured at 1 Sun intensity corresponds to the drop in IPCE measured at low light intensity, the decrease in I_{SC} likely arises from the photoelectrode degradation instead of charge carrier losses in the electrolyte. The fact that the charge carrier losses during the aging were minor enough to not largely affect the cell resistances measured with EIS (Figure 5B and C) also defends the conclusion.

A study in literature hypothesizes that the electron injection efficiency decreased when water was introduced to the cell [25], because the increased TiO_2 conduction band edge prevents electrons from moving from the LUMO level of the dye to the conduction band of the TiO_2. This phenomenon may well be wavelength dependent: photons with shorter wavelengths are more likely to excite electrons to higher energy levels of the dye, which allows them to move from the dye to the TiO_2 layer more often than electrons excited by longer wavelength photons. Water was added to the electrolyte purposely in that study [26], whereas in this study the water was introduced due to the penetration via the sealant. Overall, water is a likely reason for the degradation in this aging test since the decrease of I_{SC} was linked to the rainy periods.

There is also another explanation for the decrease of I_{SC} and IPCE: The electron collection efficiency is lower

© 2018 The Authors. *Energy Science & Engineering* published by the Society of Chemical Industry and John Wiley & Sons Ltd.

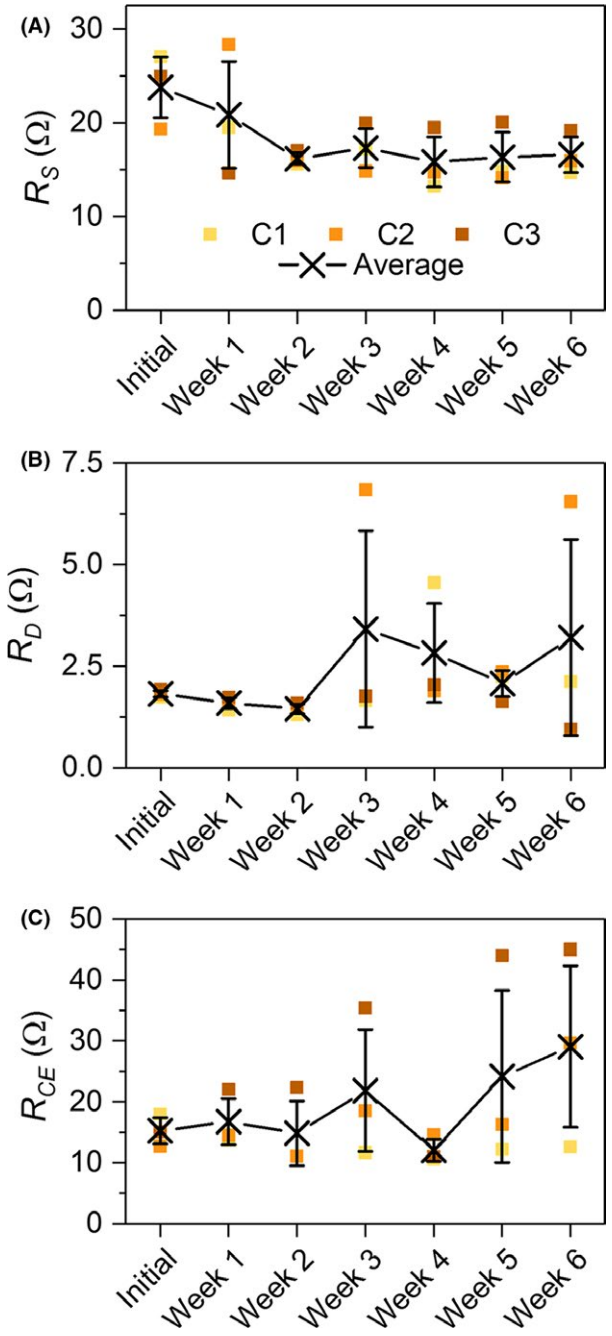

Figure 5. The figure shows (A) series resistances of the cell, (B) mass transport resistance of electrolyte at the counter electrode, and (C) charge transfer resistance at the counter electrode-electrolyte interface acquired from the equivalent circuit fits to the electrochemical impedance spectroscopy results. High variance in some values is most likely due to failed fitting of equivalent circuit to the spectrum.

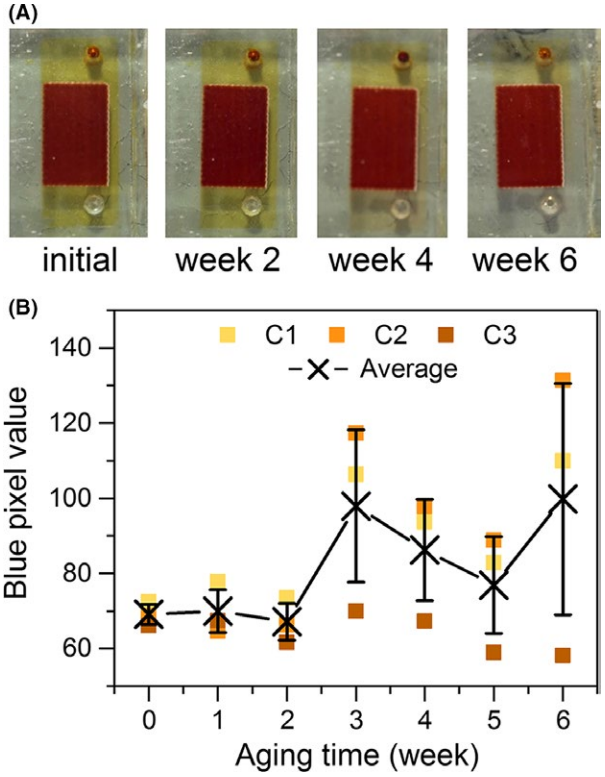

Figure 6. (A) Cell 2 photographed from throughout the test period. (B) Average blue pixel values of the electrolyte of all cells. The yellow electrolyte color originates from the amount of iodine in the electrolyte. The higher blue pixel value for the electrolyte, the more the electrolyte has bleached indicating loss of iodine. The electrolyte in the cells bleaches during the aging as shown in the photo (A) and in the analyzed electrolyte color (B).

for electrons excited by longer wavelengths: longer wavelengths penetrate deeper into the cell than shorter wavelengths. For that reason, the electrons generated by long wavelength photons have longer distance to the external circuit and thus have higher chance for recombination. If the amount of recombination sites increased, the electrons generated by long wavelength photons are more likely to encounter the additional recombination sites, which explain why the IPCE has decreased more in the longer wavelength region. Lastly, the dye molecules may have also degraded due to chemical changes, for example, due to impurities from the rainwater. It is possible that a part of the dye molecule transforms into other form, which may alter how the molecule responds to light, which has an impact on light harvesting efficiency. This alternative theory does not exclude the theory of band shifting and in fact, I_{SC} may have decreased due to a combined effect.

Outdoor measurements

The section *Indoor measurements* demonstrate that all the tested cells behaved similarly during the aging test. Therefore, for the sake of clarity, we show in this section the outdoor measurement data only for one cell (C1).

© 2018 The Authors. *Energy Science & Engineering* published by the Society of Chemical Industry and John Wiley & Sons Ltd.

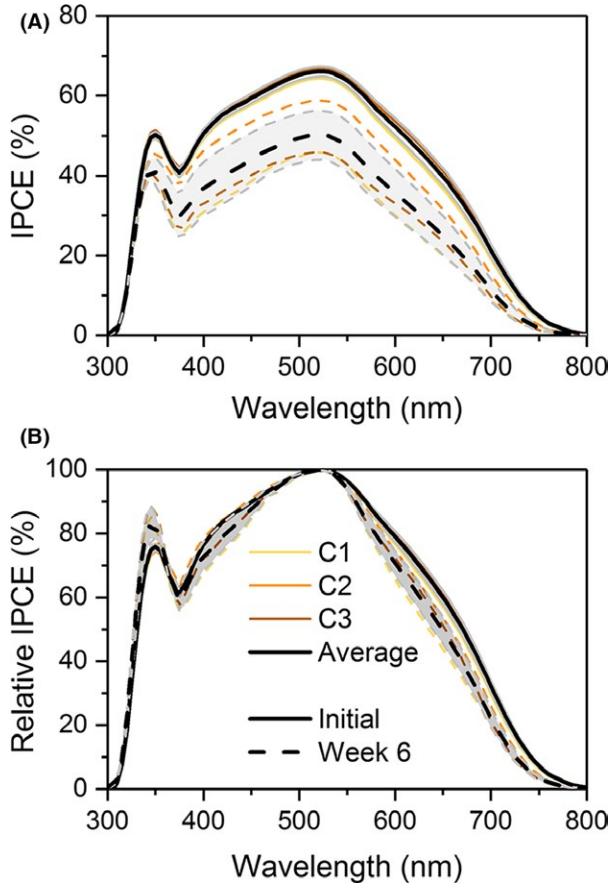

Figure 7. (A) Absolute and (B) normalized incident photon to collected electron spectra of the cells. Initial and post-aging measurements are plotted with solid and dashed lines, respectively. The grayed area represents the standard deviation of the final results. The absolute IPCE has reduced during aging (fig part A) and the decrease is the largest at high wavelengths (fig part B).

The outdoor IV data of Figure 8 shows time development similar to the indoor measurements: V_{OC} increases slightly and η and power density decrease slightly. The losses to the latter were most likely due to the reduction of photocurrent generation, which was evident from Figure 4 but difficult to interpret from Figure 8 alone. *FF* is lower at high light intensities and higher at low intensities because the larger current produced under higher intensity illumination produces larger losses due to cell resistances.

The data in Figure 8 shows an interesting finding that the cells appear to operate quite similarly in freezing conditions, even near −10°C, than in non-freezing conditions. There is no clear drop in any of the IV parameters between 670 and 950 h when it was freezing. During that period, on the cloudy days, the cell temperature remained below zero throughout the day but on the sunnier days (near 750 and 875 h) the Sun heated the cells to temperatures between 5°C and 15°C (high variations were observed due to clouds and wind gusts on those days).

The typical efficiency in outdoor conditions was relatively high, around 10i% (Fig. 8). This is about twice as high as the values in indoors measurement under 1 Sun illumination (Fig. 4). The reason for this is that typical outdoor irradiance remained well below 100 W/m^2. With such low intensities, the current generation is low and the resistive losses are small which increases *FF* and η. Overall, the current and power densities of the cell in Figure 8 are quite well linearly and directly proportional to the light intensity. On the contrary, both η and *FF* are inversely proportional. V_{OC} is expectedly relatively independent on light intensity with irradiances above 10 W/m^2 (Fig. 8) and increased only slightly for high intensities.

η and the maximum power density of the cell are plotted as a function of light intensity into Figure 9A and B and their correlation relations are shown in Table 3. η was much higher for lower intensities and slightly higher for early scans due to degradation during aging. Interestingly, the variance of η is much higher at low intensities. This is most likely due to inaccuracy of parameter estimation from the IV scans because the absolute errors related to accuracy of both the current and the light intensity measurement stay constant with respect to the measured value. Power density is nearly linearly dependent on light intensity. The consecutive scans (especially the high-intensity scans close to the beginning of the aging test) show nearly linear increase when the Sun was rising or setting during a clear sky day.

We investigated the relations of the different weather conditions to the cell performance. The immediate efficiency of the cell seems to be statistically independent of both temperature and humidity since there are no clearly visible trends in Figure 9C and D and the R^2 value is very low in both cases, see Table 3. Actually, the weather parameters were more dependent on each other (figures not shown here). For example, when sun was shining, it was warmer and dryer. Since high irradiance decreases the cell efficiency, it would seem that the higher temperature and lower humidity decrease η unless the irradiance is taken into account. The connected weather parameters make the relations of the parameters and the cell efficiency much more complicated to analyze because a simple linear model does not apply. Therefore, more advanced statistical analysis is needed for investigating in detail the effect of temperature and humidity on cell efficiency. Literature comments that making such correlations, in practice estimating the acceleration factor of aging, for test in which there are multiple aging factors present is very difficult or even impossible in practice [27, 28]. Therefore, separate indoor

© 2018 The Authors. *Energy Science & Engineering* published by the Society of Chemical Industry and John Wiley & Sons Ltd.

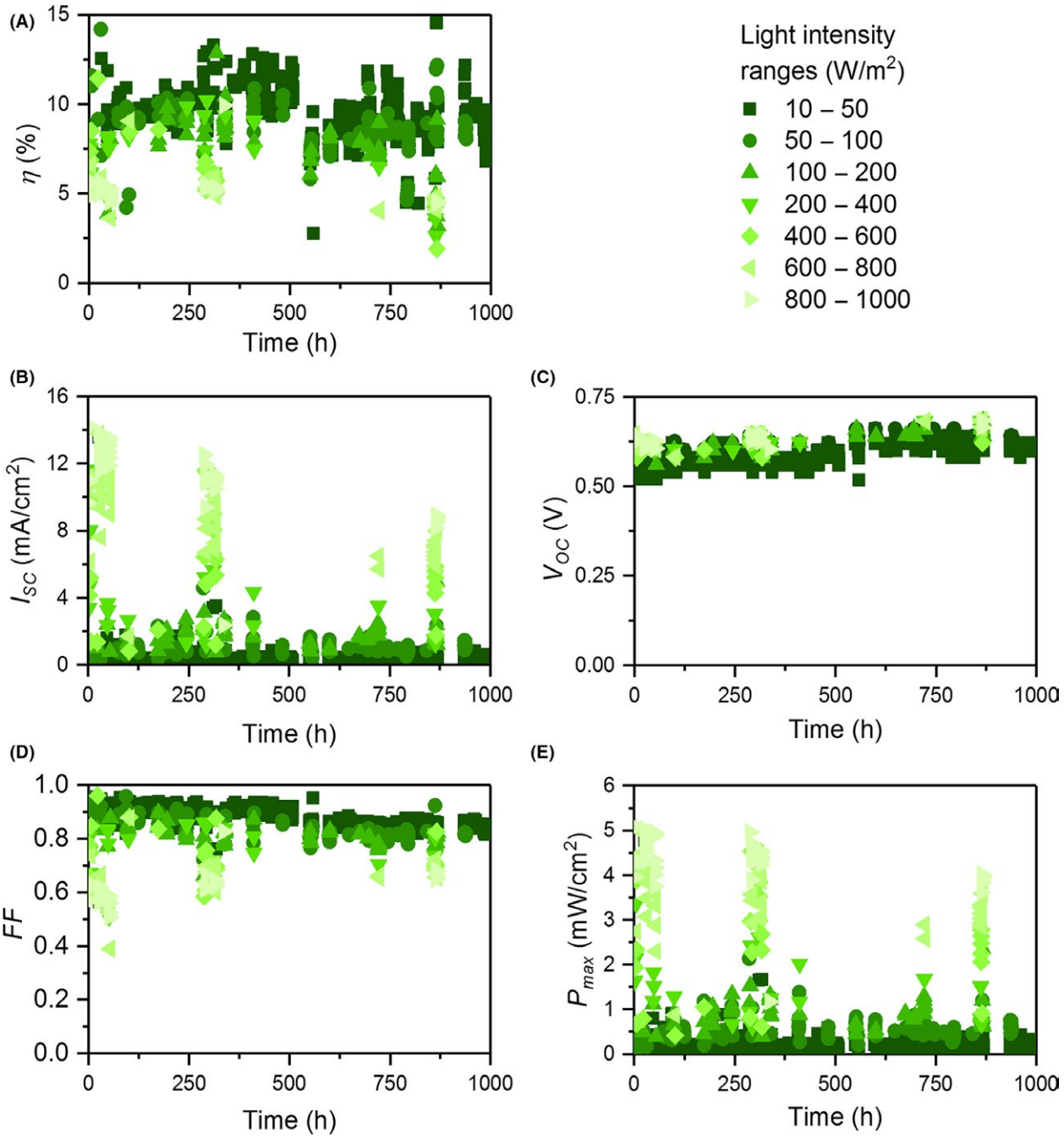

Figure 8. (A) Efficiency, (B) short circuit current density, (C) open circuit voltage (D) fill factor, and (E) maximum power density over the outdoor test period for cell C1. The lighter green the color of the data points the higher is the light intensity during the current-voltage scan. Between 670 and 950 h the ambient temperature was freezing. With the lowest light intensities, the cell reaches the highest efficiencies as the fill factor losses are reduced to their minimum values.

test measurements with fixed light intensity, temperature, and humidity levels would be needed for revealing the actual empirical relation of cell efficiency to the environment parameters. However, both cases are beyond the scope of this work.

The cells were aged in open circuit conditions but Figure 10 shows the theoretical cumulative energy generation of the example cell C1. The cumulative energy generation was calculated by integrating the maximum power point values obtained from the outdoor IV

© 2018 The Authors. *Energy Science & Engineering* published by the Society of Chemical Industry and John Wiley & Sons Ltd.

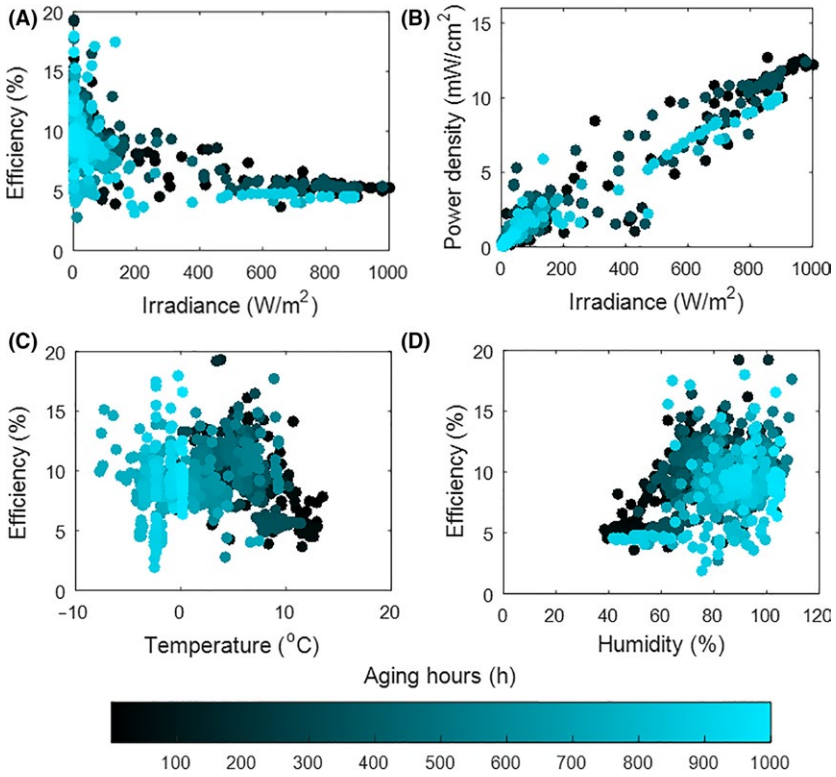

Figure 9. (A) Efficiency and (B) maximum power density as a function of irradiance. Efficiency as a function of (C) temperature and (D) humidity. Data is from cell C1. The data point color show the scan time of the data point. Irradiance has an effect on efficiency and power density as to be expected. Instead temperature does show a relation with efficiency. Humidity and temperature show some correlation, but this is most likely due to how the environmental parameters link: humidity is low when irradiance is high and the efficiency gets lower with higher irradiance.

measurements over time. Next, the theoretical cumulative efficiency of the cell was determined by calculating the ratio for cumulative power output and irradiance. This value describes the proportion of the total solar irradiance during the aging test that the cell could have converted into electricity during the test period (assuming that the aging phenomena of the cells remain the same at open circuit or under load). It is noteworthy that the cumulative efficiency (Fig. 10) is higher than the one obtained from the indoor IV characterizations (Fig. 4). The cells perform better in the actual outdoor conditions than under simulated 1 Sun AM 1.5 G illumination. The cell described in this section produced about 50% higher average η compared to the indoors measurement at standard conditions. When comparing to C-Si solar cells, an opposite behavior is seen: when the illumination decreases from 1 Sun to 0.001 Sun, the efficiency of c-Si cells gets halved [2]. The good performance of DSSCs under low light conditions compared to conventional solar cells is their known characteristic and recently DSSCs have reach as high as 28.9% efficiency under ambient indoor light conditions [1].

Table 3. Statistical correlation parameters of efficiency, power density, and weather parameters. The equation is for the linear fit into the variable pair and the R^2 value describe the goodness of the fit (0 bad fit, 1 perfect fit). In the variable pair the left variable is the explanatory variable (x) and the right one dependent variable (y). The units for variables are the same as in Figure 9.

Variable pair		Equation	R^2 value
Irradiance	Efficiency	$y = -0.006x + 9.98$	0.36
Irradiance	Power density	$y = 0.012x + 0.31$	0.89
Temperature	Efficiency	$y = 0.012x + 9.33$	0.0005
Humidity	Efficiency	$y = 0.055x + 4.89$	0.12
Irradiance	Temperature	$y = 0.006x + 2.56$	0.10
Irradiance	Humidity	$y = -0.046x + 86.8$	0.45
Temperature	Humidity	$y = -1.576x + 87.37$	0.21

Conclusions

Here we report an outdoor test of dye-sensitized solar cells in northern climate conditions. This was highly motivated since there are only few outdoor studies for dye solar cells reported in literature and this is the first one tracking performance in Nordic outdoor conditions. The 6-week (1000 h) aging test took place in late autumn.

© 2018 The Authors. *Energy Science & Engineering* published by the Society of Chemical Industry and John Wiley & Sons Ltd.

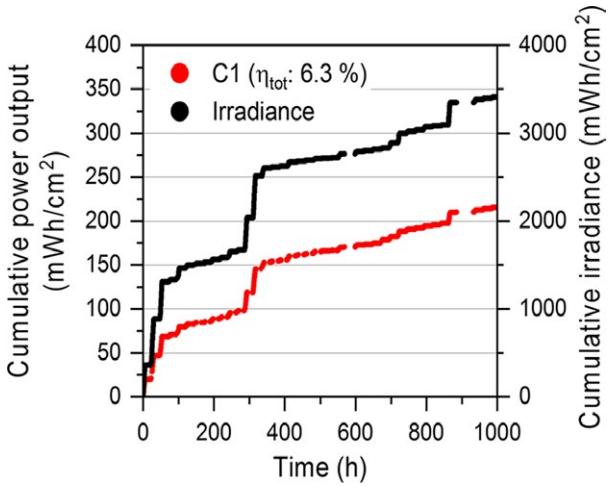

Figure 10. The cumulative energy generation of cell C1 and the cumulative irradiance during the outdoor aging test. The small gaps in the data are due to either cell contact failure or system failure. The efficiency visible in the legend (η_{tot}) describes how large share of the cumulative irradiance the cell could have converted to electricity were it aged under load. It should be noted that here η_{tot} was 50% higher compared to η at standard reporting conditions.

The weather varied from +10°C and sunny to +5°C and rainy to −5°C and snowy. The tested cells showed degradation only during rainy and non-freezing conditions, so rainwater seems to be the most likely source of degradation. The cell performance remained stable when the cells were exposed to freezing temperatures and furthermore, the cells were able to produce power under these freezing conditions about as well as in above zero temperature.

The cells maintained their efficiency quite well to the end of the test (88%) and the minor decrease was mostly due to decreased current generation. The IPCE showed a loss corresponding to the loss seen in photocurrent production. Hence, the loss of photocurrent was namely related to changes at the photoelectrode, such as the degradation of the dye, and was not limited by the charge transfer properties of the electrolyte. It is, however, important to notice that there was also a significant loss of tri-iodide charge carriers (about 50%), which did not (yet, due to initial excess of tri-iodide) limit the photocurrent production at 1 Sun and caused only minor losses to the device performance. The tri-iodide loss rate was, however, so significant that it would soon have become a major loss factor and would have eventually caused the ultimate cell failure. When looking at improving the device lifetime, the loss of charge carriers should be a top priority. This shows how important it is to look beyond cell efficiency and its degradation rate and find deeper insight by the quantitative analysis of the loss mechanisms and their rates.

The outdoor data revealed that below 100 W/m^2 illumination, the cells were remarkably about twice as efficient as under 1000 W/m^2 illumination, reaching about 10% efficiencies. This is because the resistive losses decreasing the fill factor reduce tremendously (over 20%) when the current provided by the cell is low. Because of the high efficiency at lower light intensities, the calculated overall light to electricity conversion efficiency of the cells reached as much as 50% higher values in comparison to the standard measurement conditions. It is noteworthy to mention that whilst the conventional silicon solar cell suffer significant losses when light intensity decreases [2], the efficiency of DSSCs increases in low light intensities.

Acknowledgments

SL thanks financial support from the Academy of Finland (project SOLID 271081), KM thanks the Kone Foundation, and AT thanks the Tiina and Antti Herlin Foundation. We thank Valeria Azovskaya / Aalto Materials Platform for photos used in Figures 1C-D.

Conflict of Interest

None declared.

References

1. Freitag, M., J. Teuscher, Y. Saygili, X. Zhang, F. Giordano, P. Liska et al. 2017. Dye-sensitized solar cells for efficient power generation under ambient lighting. Nat. Photonics 11:372–378.
2. Ruhle, K., M. K. Juhl, M. D. Abbott, and M. Kasemass. 2015. Evaluating crystalline silicon solar cells at low light intensities using intensity-dependent analysis of I-V parameters. IEEE J. Photovolt. 5:926–931.
3. Cornaro, C., S. Bartocci, D. Musella, C. Strati, A. Lanuti, S. Mastroianni et al. 2015. Comparative analysis of the outdoor performance of a dye solar cell mini-panel for building integrated photovoltaics applications. Prog. Photovolt. 23:215–225.
4. Hinsch, A., H. Brandt, W. Veurman, S. Hemming, M. Nittel, U. Würfel et al. 2009. Dye solar modules for façade applications: recent results from project ColorSol. Sol. Energy Mat. Sol. Cells 93:820–824.
5. Asghar, M. I., K. Miettunen, J. Halme, P. Vahermaa, M. Toivola, K. Aitola et al. 2010. Review of stability for advanced dye solar cells. Energy Environ. Sci. 3:418–426.
6. Asghar, M. I., K. Miettunen, S. Mastroianni, J. Halme, H. Vahlman, and P. Lund. 2012. In situ image processing method to investigate performance and stability of dye solar cells. Sol. Energy 86:331–338.
7. Berginc, M., U. O. Krašovec, and M. Topič. 2014. Outdoor ageing of the dye-sensitized solar cell under

© 2018 The Authors. *Energy Science & Engineering* published by the Society of Chemical Industry and John Wiley & Sons Ltd.

different operation regimes. Sol. Energy Mat. Sol. Cells 120:491–499.
8. Mastroianni, S., A. Lanuti, S. Penna, A. Reale, T. M. Brown, A. Di Carlo et al. 2012. Physical and electrochemical analysis of an indoor–outdoor ageing test of large-area dye solar cell devices. ChemPhysChem 13:2925–2936.
9. Bella, F., G. Griffini, M. Gerosa, S. Turri, and R. Bongiovanni. 2015. Performance and stability improvements for dye-sensitized solar cells in the presence of luminescent coatings. J. Power Sources 283:195–203.
10. Tanaka, H., A. Takeichi, K. Higuchi, T. Motohiro, M. Takata, N. Hirota et al. 2009. Long-term durability and degradation mechanism of dye-sensitized solar cells sensitized with indoline dyes. Sol. Energy Mat. Sol. Cells 93:1143–1148.
11. Kato, N., K. Higuchi, H. Tanaka, J. Nakajima, T. Sano, and T. Toyoda. 2011. Improvement in long-term stability of dye-sensitized solar cell for outdoor use. Sol. Energy Mat. Sol. Cells 95:301–305.
12. Knag, J.-G., J.-H. Kim, H.-B. Jang, and J.-T. Kim. 2015. Characteristics of DSSC panels with silicone encapsulant. Int. J. Photoenergy 2015:715427.
13. Ivanou, D. K., R. Santos, J. Maçaira, L. Andrade, and A. Mendes. 2016. Laser assisted glass frit sealing for production large area DSCs panels. Sol. Energy 135:674–681.
14. Kato, N., Y. Takeda, K. Higuchi, A. Takeichi, E. Sudo, H. Tanaka et al. 2009. Degradation analysis of dye-sensitized solar cell module after long-term stability test under outdoor working condition. Sol. Energy Mat. Sol. Cells 93:893–897.
15. Dai, S., J. Weng, Y. Sui, S. Chen, S. Xia, Y. Huang et al. 2008. The design and outdoor application of dye-sensitized solar cells. Inorg. Chim. Acta 361:786–791.
16. Toyoda, T., T. Sano, J. Nakajima, S. Doi, S. Fukumoto, A. Ito et al. 2004. Outdoor performance of large scale DSC modules. J. Photochem. Photobiol. A Chem. 164:203–207.
17. Asghar, A., M. Emziane, H. K. Pak, and S. Y. Oh. 2014. Outdoor testing and degradation of dye-sensitized solar cells in Abu Dhabi. Sol. Energy Mat. Sol. Cells 128:335–342.
18. Dong, Q., F. Liu, M. K. Wong, H. W. Tam, A. B. Djurišić, A. Ng et al. 2016. Encapsulation of perovskite solar cells for high humidity conditions. Chemsuschem 9:2579–2603.
19. Li, X., M. Tschumi, H. Han, S. S. Babkair, R. A. Alzubaydi, A. A. Ansari et al. 2015. Outdoor performance and stability under elevated temperatures and long-term light soaking of triple-layer mesoporous perovskite photovoltaics. Energy Technol. 3:551–555.
20. Reese, M. O., S. A. Gevorgyan, M. Jørgensen, E. Bundgaard, S. R. Kurtz, D. S. Ginley et al. 2011. Consensus stability testing protocols for organic photovoltaic materials and devices. Sol. Energy Mat. Sol. Cells 95:1253–1267.
21. Mastroianni, S., I. Asghar, K. Miettunen, J. Halme, A. Lanuti, T. M. Brown et al. 2014. Effect of electrolyte bleaching on the stability and performance of dye solar cells. Phys. Chem. Chem. Phys. 16: 6092–6100.
22. Zhang, Z., S. Ito, J.-E. Moser, S. M. Zakeeruddin, and M. Grätzel. 2009. Influence of iodide concentration on the efficiency and stability of dye-sensitized solar cell containing non-volatile electrolyte. ChemPhysChem 10:1834–1838.
23. Jung, Y.-S., B. Yoo, M. K. Lim, S. Y. Lee, and K.-J. Kim. 2009. Effect of Triton X-100 in water-added electrolytes on the performance of dye-sensitized solar cells. Electrochem. Acta 54:6286–6291.
24. Zhu, K., S. R. Jang, and A. J. Frank. 2012. Effects of water intrusion on the charge-carrier dynamics, performance, and stability of dye-sensitized solar cells. Energy Environ. Sci. 5:9492–9495.
25. Carnie, M., D. Bryant, T. Watson, and D. Worsley. 2012. Photocatalytic oxidation of triiodide in UVA-exposed dye-sensitized solar cells. Int. J. Photoenergy 524590:8.
26. Hahlin, M., E. M. J. Johansson, R. Schölin, H. Siegbahn, and H. Resnmo. 2011. Influence of water on the electronic and molecular surface structures of Ru-dyes at nanostructured TiO_2. J. Phys. Chem. C 115:11996–12004.
27. Haillant, O., D. Dumbleton, and A. Zielnik. 2011. An Arrhenius approach to estimating organic photovoltaic module weathering acceleration factors. Sol. Energy Mat. Sol. Cells 95:1889–1895.
28. McMahon, T. J., G. J. Jorgensen, R. L. Hulstrom, D. L. King, and M. A. Quintana. 2000. Module 30 year life: what does it mean and is it predictable/achievable?. National Center for Photovoltaics Program Review Meeting.
29. Elevation data from: elevationmap.net; viewed on November 24th 2016.
30. Global Solar Atlas. Available at http://globalsolaratlas.info/ (accessed 22 August 2017).
31. Climate descriptions for study cities from Wikipedia: en.wikipedia.org; viewed on November 24th 2016.

 © 2018 The Authors. *Energy Science & Engineering* published by the Society of Chemical Industry and John Wiley & Sons Ltd.